

Softmax parameterization of the occupation numbers for natural orbital functionals based on electron pairing approaches

Lizeth Franco,[†] Iván A. Bonfil-Rivera,[†] Juan Felipe Huan Lew-Yee,^{*,‡} Mario Piris,^{*,‡,¶,§} Jorge M. del Campo,^{*,†} and Rodrigo A. Vargas-Hernández^{*,||,⊥}

[†]*Departamento de Física y Química Teórica, Facultad de Química, Universidad Nacional Autónoma de México, México City, C.P. 04510, México*

[‡]*Donostia International Physics Center (DIPC), 20018 Donostia, Spain.*

[¶]*Kimika Fakultatea, Euskal Herriko Unibertsitatea (UPV/EHU), 20018 Donostia, Spain.*

[§]*IKERBASQUE, Basque Foundation for Science, 48013 Bilbao, Spain.*

^{||}*Department of Chemistry and Chemical Biology, McMaster University, Hamilton, ON, Canada*

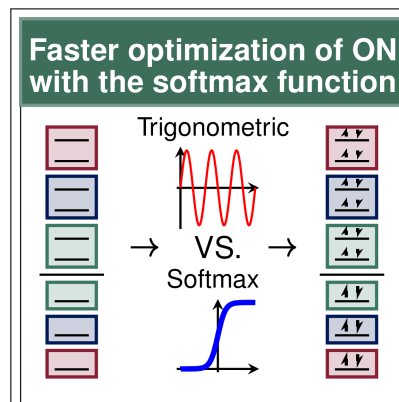
[⊥]*Brockhouse Institute for Materials Research, McMaster University, Hamilton, ON, Canada*

E-mail: felipe.lew.yee@dipc.org; mario.piris@ehu.eus; jmdelc@unam.mx; vargashr@mcmaster.ca

Abstract

Within the framework of natural orbital functional theory, having a convenient representation of the occupation numbers and orbitals becomes critical for the computational performance of the calculations. Recognizing this, we propose an innovative parametrization of the occupation numbers that takes advantage of the electron-pairing approach used in Piris natural orbital functionals through the adoption of the softmax function, a pivotal component in modern deep-learning models. Our approach not only ensures adherence to the N-representability of the first-order reduced density matrix (1RDM) but also significantly enhances the computational efficiency of 1RDM functional theory calculations. The effectiveness of this alternative parameterization approach was assessed using the W4-17-MR molecular set, which demonstrated faster and more robust convergence compared to previous implementations.

TOC Graphic



Keywords

Optimization, Occupation Numbers, activation function, machine learning, PNOF, PyNOF, W4-17-MR.

Introduction

Reduced-density-matrix-based methods promise higher accuracy compared to density functional approximations while being computationally less demanding than wavefunction methods.¹ In particular, one-electron reduced density matrix functional theory (1RDMFT) is rooted in Gilbert’s extension² of the Hohenberg-Kohn theorem,³ further developed through the efforts of Levy⁴ and Valone,⁵ who demonstrated the existence of an exact, yet undiscovered, functional of the first-order reduced density matrix (1RDM). On the other hand, Coleman’s seminal work⁶ underscored the importance of constraining the 1RDM to be N-representable, which can be achieved by restricting its eigenvalues within the zero to one interval, and ensuring that its sum equals the total number of electrons.⁷ In the natural orbital (NO) representation, the 1RDM becomes diagonal, with the occupation numbers (ONs) being its eigenvalues. The conditions for the ONs can be cast as follows:

$$0 \leq n_i \leq 1, \text{ and } \sum_i n_i = N, \quad (1)$$

where n_i is the ON of the i^{th} -NO, N is the total number of electrons, and the sum goes over all spin natural orbitals. This led to the development of functionals based on NOs and their ONs, transforming the 1RDMFT into a natural orbital functional theory (NOFT).^{8–12} At this point, it is worth acknowledging that the investigation of the 1RDM functional remains an active research field with promising applications by itself,^{13–19} while its advances can directly benefit the development of NOFT. On the other hand, we also advise the reader to consult a recent review article to obtain a comprehensive historical account of the formulation and development of NOFT.²⁰

Routine NOF calculations frequently involve simultaneous or alternate optimization of NOs and their ONs. For this reason, the development of effective optimization schemes plays a critical role in facilitating the widespread adoption of NOFT in quantum chemistry sim-

ulations. Orbital optimization can be performed using iterative diagonalization,²¹ and orbital rotations,^{22,23} while several approaches have been proposed to perform ON optimization in an unconstrained manner while preserving Eq. (1) conditions.^{24–26} For example, Yao *et al.*^{27,28} recently proposed an explicit by implicit (EBI)^{27,28} representation of ONs, stimulating various creative approaches to deal with convergence.^{29,30} The EBI method is notable for its provision of a conducive surface for auxiliary optimization parameters, representing a significant advancement in ON optimization.

In line with various electronic structure methods, RDMs have been integrated into machine learning frameworks, for example, to evaluate the energies and atomic forces of small molecules.³¹ In addition, convolutional neural networks have been used in the prediction of 2RDM’s eigenvalues.^{32,33} The present work is directly inspired by these developments. However, we took a different approach, aiming to harness the softmax activation function utilized in machine learning models,^{34,35} to parameterize ONs in a manner that satisfies Eq. (1). Our approach is rooted in the belief that the integration of machine learning techniques with NOFT can lead to significant improvements in solving convergence issues, thereby enhancing its applicability and effectiveness in quantum chemistry RDM-based simulations.

Methods

Recent advances in the field of NOFT have been marked by the development of electron-pairing-based Piris NOFs (PNOFs).^{36–39} PNOFs have shown remarkable performance in addressing the charge delocalization error,^{40,41} and handling challenging multireference problems.^{42–45} The latest addition to this family is the Global NOF,⁴⁶ which aims to strike a balance between static and dynamic electron correlation. In particular, it represents a promising approach with manageable computational demands,⁴⁷ highlighting the importance of ongoing development and motivating the exploration of new convergence schemes that can benefit these methodologies.

In the following, we consider N_I unpaired electrons, which determine the total spin of the system, S . The remaining electrons, $N_{II} = N - N_I$, form pairs with opposite spins, resulting in a net spin of zero for N_{II} electrons combined. For the equally mixed state of highest multiplicity, defined by $2S + 1 = N_I + 1$,⁴⁸ the expected value of \hat{S}_z is zero. Consequently, restricted spin theory is applied: $\varphi_p^\alpha(\mathbf{r}) = \varphi_p^\beta(\mathbf{r}) = \varphi_p(\mathbf{r})$, $n_p^\alpha = n_p^\beta = n_p$.

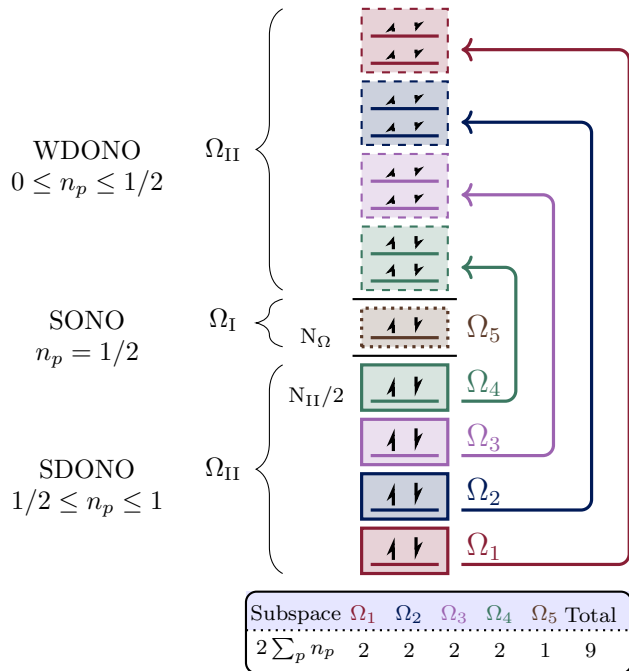


Figure 1: Splitting of the orbital space Ω into subspaces for a system with nine electrons in a doublet spin state ($N_I=1$, $2S+1=2$). In this example, one orbital make up the subspace $\Omega_I=\Omega_5$, whereas eight electrons ($N_{II} = 8$) distributed in four subspaces $\{\Omega_1, \Omega_2, \Omega_3, \Omega_4\}$ make up the subspace Ω_{II} . Note that $N_g=2$ for all subspaces $\Omega_g \in \Omega_{II}$. The arrows depict the values of the ensemble occupancies, alpha (\downarrow) or beta (\uparrow), in each orbital $|p\rangle$.

The orbital space Ω is divided into disjoint subspaces $\Omega_g = \{\varphi_g, \varphi_1, \varphi_2, \dots, \varphi_{N_g}\}$, which leads to explicit terms for intra and inter-pair electron correlation.⁴⁹ The value of N_g may vary for each subspace, with its maximum determined by the basis set. An illustration of Ω can be seen in Fig. 1, depicting the case of a doublet system with nine electrons and $N_g = 2$. There are

four strongly double-occupied NOs (SDONO), each coupled with two weakly double-occupied NOs (WDONO), comprising the subspace Ω_{II} distributed in four subspaces $\{\Omega_1, \Omega_2, \Omega_3, \Omega_4\}$. Taking into account the spin, the total occupancy for a given subspace in Ω_{II} is 2, which is reflected in the following pairing condition sum rule for the orbitals of a given spin,

$$\sum_{p \in \Omega_g} n_p = n_g + \sum_{i=1}^{N_g} n_{p_i} = 1; g = 1, \dots, \frac{N_{II}}{2}. \quad (2)$$

In addition, the single occupied NO (SONO) in Ω_5 belongs to Ω_I and is responsible for the doublet state. It is important to emphasize that each orbital in Ω_I accommodates a single electron ($n_p = \frac{1}{2}$), but the specific spin state, whether α or β , is unknown.

The electron-pairing strategy effectively converts the normalization condition into multiple sum rules designed for electron pairs, as shown in Eq. (2), ensuring the inherent fulfillment of Eq. (1),

$$2 \sum_{p \in \Omega} n_p = 2 \left(\sum_{p \in \Omega_I} + \sum_{p \in \Omega_{II}} \right) n_p = N_I + N_{II} = N. \quad (3)$$

In the following, we review the current state-of-the-art of occupation number parameterization by trigonometric functions in the context of electron-pairing NOFs, then, we present a parameterization based on the softmax function. For this work's context, the goal is to promote the use of the `softmax` function⁵⁰ as an alternative parametrization of the ONs while leveraging the electron-pairing conditions [Eq. (2)] employed in PNOF.

Trigonometric parameterization

A notable aspect of the orbital pairing approach is that it directly enables unconstrained minimization of the ONs, which is particularly advantageous for optimization in NOFT. This has long been performed employing trigonometric functions.²⁵ In the specific case at hand, the ONs can be represented by means of squared trigonometric functions. For a subspace Ω_g , the

occupation number n_g of the SDONO is given by

$$n_g = \frac{1}{2} (1 + \cos^2 \gamma_g), \quad g = 1, \dots, \frac{N_{\text{II}}}{2}, \quad (4)$$

while the occupation number of the WDONOs, n_{p_i} , are given by,

$$\begin{aligned} n_{p_1} &= h_g \sin^2 \gamma_{p_1}, \\ n_{p_2} &= h_g \cos^2 \gamma_{p_1} \sin^2 \gamma_{p_2}, \\ &\vdots \\ n_{p_i} &= h_g \cos^2 \gamma_{p_1} \cos^2 \gamma_{p_2} \cdots \cos^2 \gamma_{p_{i-1}} \sin^2 \gamma_{p_i}, \\ &\vdots \\ n_{p_{N_g-1}} &= h_g \cos^2 \gamma_{p_1} \cos^2 \gamma_{p_2} \cdots \cos^2 \gamma_{p_{N_g-2}} \sin^2 \gamma_{p_{N_g-1}}, \\ n_{p_{N_g}} &= h_g \cos^2 \gamma_{p_1} \cos^2 \gamma_{p_2} \cdots \cos^2 \gamma_{p_{N_g-2}} \cos^2 \gamma_{p_{N_g-1}}, \end{aligned} \quad (5)$$

where $h_g = 1 - n_g$. It can be easily shown that the pairing condition in Eq. (2) is inherently guaranteed by the Pythagorean trigonometric identity.²⁶

Analytic gradients for the occupation numbers, with respect to the auxiliary variables, can be directly obtained as follows,

$$\begin{aligned} \frac{dn_g}{d\gamma_g} &= -\frac{1}{2} \sin(2\gamma_g), \quad g = 1, \dots, \frac{N_{\text{II}}}{2}, \\ \frac{\partial n_{p_i}}{\partial \gamma_g} &= -\frac{dn_g}{d\gamma_g} \cos^2 \gamma_{p_1} \cdots \cos^2 \gamma_{p_{i-1}} \sin^2 \gamma_{p_i}, \quad p_i \in \Omega_g, \\ \frac{\partial n_{p_i}}{\partial \gamma_{p_j}} &= -h_g \cos^2 \gamma_{p_1} \cdots \sin 2\gamma_{p_j} \cdots \cos^2 \gamma_{p_{i-1}} \sin^2 \gamma_{p_i}, \quad j < i \neq N_g, \\ \frac{\partial n_{p_i}}{\partial \gamma_{p_i}} &= h_g \cos^2 \gamma_{p_1} \cdots \cos^2 \gamma_{p_{i-1}} \sin 2\gamma_{p_i}, \quad i \neq N_g, \\ \frac{\partial n_{p_i}}{\partial \gamma_{p_j}} &= -h_g \cos^2 \gamma_{p_1} \cdots \cos^2 \gamma_{p_{i-1}} \sin 2\gamma_{p_i}, \quad j < i = N_g. \end{aligned} \quad (6)$$

Overall, the parameterization effectively transforms the optimization of the ONs into a minimization of the unbounded auxiliary variables (γ_p). However, since this parameterization involves the product of trigonometric functions in both the ONs and their gradients, minor deviations in γ_p values can lead to inconvenient oscillatory propagation of the error, potentially causing numerical instabilities during the simulations. These deviations are amplified as the number of orbitals in a subspace increases because of the involvement of more products of trigonometric functions (Fig. 2). In practice, this parameterization performs well when there are few coupled NOs. It is worth

acknowledging that this approach has greatly facilitated successful PNOF calculations across diverse complex systems, playing a significant role in its ongoing development.

Softmax parameterization

Higher accuracy is demanded in electronic structure calculations, so larger basis sets are required, resulting in more NOs for each subspace. Therefore, developing a more stable parameterization for the ONs becomes imperative. The softmax function can fulfill the pairing condition of Eq. (2), providing a better way to take advantage of these properties with a function defined with simple elementary functions on all parts of the domain, making it easier to implement and evaluate. Moreover, this function is commonly used in deep learning models as it parameterizes a probability distribution over multiple classes,^{34,35,50} and was also used for the alchemy design of organic electronic materials.⁵¹

Given a subspace Ω_g and using the softmax function, the ON can be parameterized as

$$n_p = \sigma(\gamma_p) = \frac{e^{\gamma_p}}{\sum_q e^{\gamma_q}}, \quad (7)$$

where p and q are the indices of NOs, that is, they can be $\{g, \{p_i\}_1^{N_g}\}$, and γ_p are auxiliary variables, also known as logits in the context of machine learning. The output of the softmax function is always normalized $\sum_p \sigma(\gamma_p) = 1$; therefore, it directly provides values for the ONs of a given subspace that fulfills Eq. (2), as opposed to other machine learning activation functions.³⁵ It is worth mentioning that the softmax function, also known as the soft-argmax or normalized exponential function,⁵⁰ is homologous to the Boltzmann distribution. Furthermore, the softmax function has closed-form gradients,^{35,50} as shown in Eq. (8). Other physically-inspired parametrizations have been proposed. For example, in Refs. 24 and 52, the ONs followed a Fermi–Dirac distribution; however, additional Lagrange multipliers were needed to satisfy Eqs. (1) and (2). It is worth noting that the framework described in

Refs. 24 and 52 is akin to the ‘‘sigmoid’’ activation function.

$$\begin{aligned} \frac{\partial n_p}{\partial \gamma_r} &= \frac{\partial \sigma(\gamma_p)}{\partial \gamma_r} \\ &= \begin{cases} \frac{e^{\gamma_p} (\sum_q e^{\gamma_q} - e^{\gamma_p})}{(\sum_q e^{\gamma_q})^2} & \text{if } r = p; \\ \frac{-e^{\gamma_p} e^{\gamma_r}}{(\sum_q e^{\gamma_q})^2} & \text{otherwise.} \end{cases} \end{aligned} \quad (8)$$

Example: A subspace with three orbitals

To better understand the performance of the ‘‘trigonometric’’ and ‘‘softmax’’ parameterizations, let us consider a subspace with a single SDONO and two WDONO for three total orbitals. This scenario enables a direct visual comparison of the two parameterization schemes. The trigonometric parameterization for three ONs is,

$$\begin{aligned} n_g &= \frac{1}{2} (1 + \cos^2 \gamma_g) \\ n_{p_1} &= (1 - n_g) \sin^2 \gamma_{p_1} \\ n_{p_2} &= (1 - n_g) \cos^2 \gamma_{p_1}, \end{aligned} \quad (9)$$

where only two γ auxiliary variables are needed to define the three ONs. Conversely, using the softmax parameterization, the ONs are

$$\begin{aligned} n_g &= \frac{e^{\gamma_g}}{e^{\gamma_g} + e^{\gamma_{p_1}} + e^{\gamma_{p_2}}} \\ n_{p_1} &= \frac{e^{\gamma_{p_1}}}{e^{\gamma_g} + e^{\gamma_{p_1}} + e^{\gamma_{p_2}}} \\ n_{p_2} &= \frac{e^{\gamma_{p_2}}}{e^{\gamma_g} + e^{\gamma_{p_1}} + e^{\gamma_{p_2}}}, \end{aligned} \quad (10)$$

where three auxiliary variables are needed to determine all three ONs.

In both approaches, the ONs are parameterized by unconstrained auxiliary variables. However, trigonometric parameterization provides surfaces that feature several valleys and hills, as shown in Fig. 2(a), where the optimizer can be trapped due to the vanishing of the gradi-

ents. Furthermore, if the optimizer takes a step slightly larger than necessary, it may transition to a different basin, invalidating prior steps and destabilizing the optimization process. In contrast, the softmax function provides a better representation of the ONs, as illustrated in Fig. 2(b), where nonoscillatory surfaces represent the three ONs. In particular, it offers a steady structure for ONs near zero and one, and a nearly linear surface for fractional ONs, which is crucial for optimizing multireference systems.

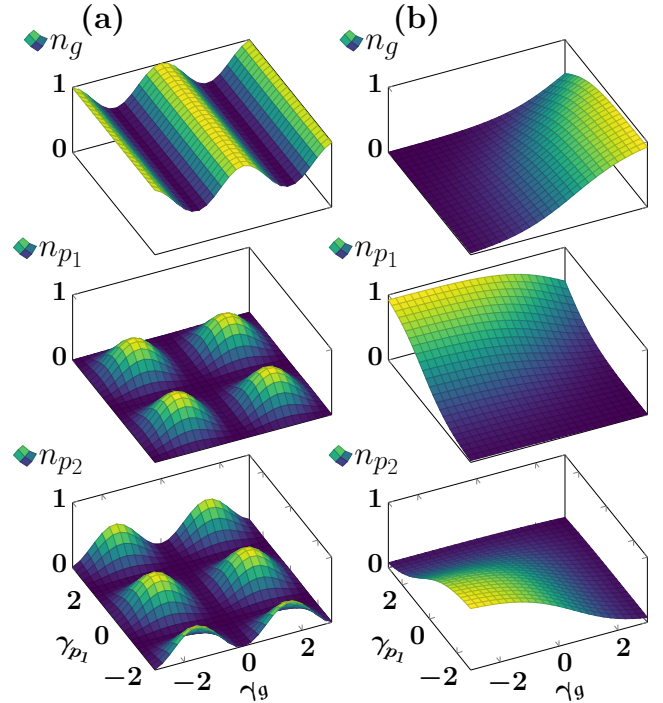


Figure 2: The value of ONs in a subspace of three NOs (n_g , n_{p_1} and n_{p_2}) as a function of the auxiliary variables (γ_p) according to (a) the trigonometric and (b) the softmax parameterizations. The softmax parameterization depends on three γ_p variables. We have fixed γ_{p_2} to $\frac{1}{2}$ for illustrative purposes.

Computational Details

All calculations were performed using the PyNOF package⁵³ with the PNOF7 functional using an extended pairing approach, employing the highest number of N_g allowed for the def2-TZVPD basis.^{54,55} The minimization procedure

was carried out with alternate optimizations of NOs and ONs, using a convergence criterion of energy change below 10^{-4} Ha for external iterations. Since the PNOF definition assigns a phase to the given strongly occupied orbital, the occupation numbers of each subspace Ω_g are automatically inspected at the end of each external iteration to ensure that its occupation number has a larger value than the occupations of the weakly occupied orbitals. If the direction of this inequality is not satisfied, the corresponding orbitals and occupation numbers are exchanged, with a negligible computational demand. The optimization of NOs was limited to 30 internal iterations using the orbital rotation method,²³ while internal iterations of ONs were performed without any specific limitation on the number of iterations, using a termination criterion of 10^{-5} for the norm of the gradient of either the trigonometric or the softmax parameterization. In both cases, the minimization has been carried out using the conjugate gradient method, with derivatives of the energy with respect to γ computed by means of the chain rule, that is, multiplying the derivatives of the energy with respect to the occupation numbers with the derivatives of the occupation numbers with respect to γ . As the purpose of this work is to study specifically the performance of the occupation number parameterization in the minimization of ONs and in the overall calculation, in the following, the optimization cycles for ONs will be termed "internal iterations", leaving aside the internal iterations of the orbital optimization, which are not relevant to the present work. On the hardware front, simulations were executed on a computer with an Intel Xeon Silver 4208 processor with 16 cores and a GPU NVIDIA GeForce RTX 4090.

Results

We benchmarked the trigonometric and softmax parameterization methods in the W4-17-MR database, which contains data for 17 multireference chemical systems.⁵⁶ These systems are characterized by significantly fractional oc-

cupation numbers, highlighting the complexity of the benchmarking cases. It is crucial to understand that the optimization process involves multiple external iterations. Each of these iterations included optimizing both the orbitals and the occupation numbers, with each step further divided into several internal iterations.

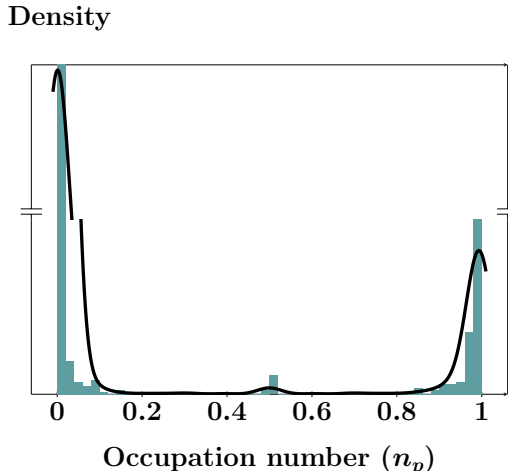


Figure 3: Normalized distribution of the occupation numbers of all molecules in the W4-17-MR dataset as obtained from PNOF7 calculations.

Figure 3 displays the ONs’ distribution across all molecules within the W4-17-MR database, revealing the necessity for specific parametrization across three distinct regimes: $n_p \approx 0$, $n_p \approx 1$, and $n_p \approx \frac{1}{2}$. This is particularly important for accurately modeling multireference systems. Both the trigonometric and softmax parameterization methods successfully capture these regimes. However, as evident from Fig. 2, the softmax function, compared to the trigonometric series, offers a wider space for the auxiliary variables (γ_p) to represent these conditions accurately.

In this regard, Fig. 4 shows the number of internal iterations required for optimizing the ONs during each external iteration and (inset panel) energy trajectory as a function of cumulative occupation iterations (COI) for all molecules of the W4-17-MR set. As we can observe, softmax parameterization demonstrates superior performance by requiring significantly fewer internal iterations than its trigonometric

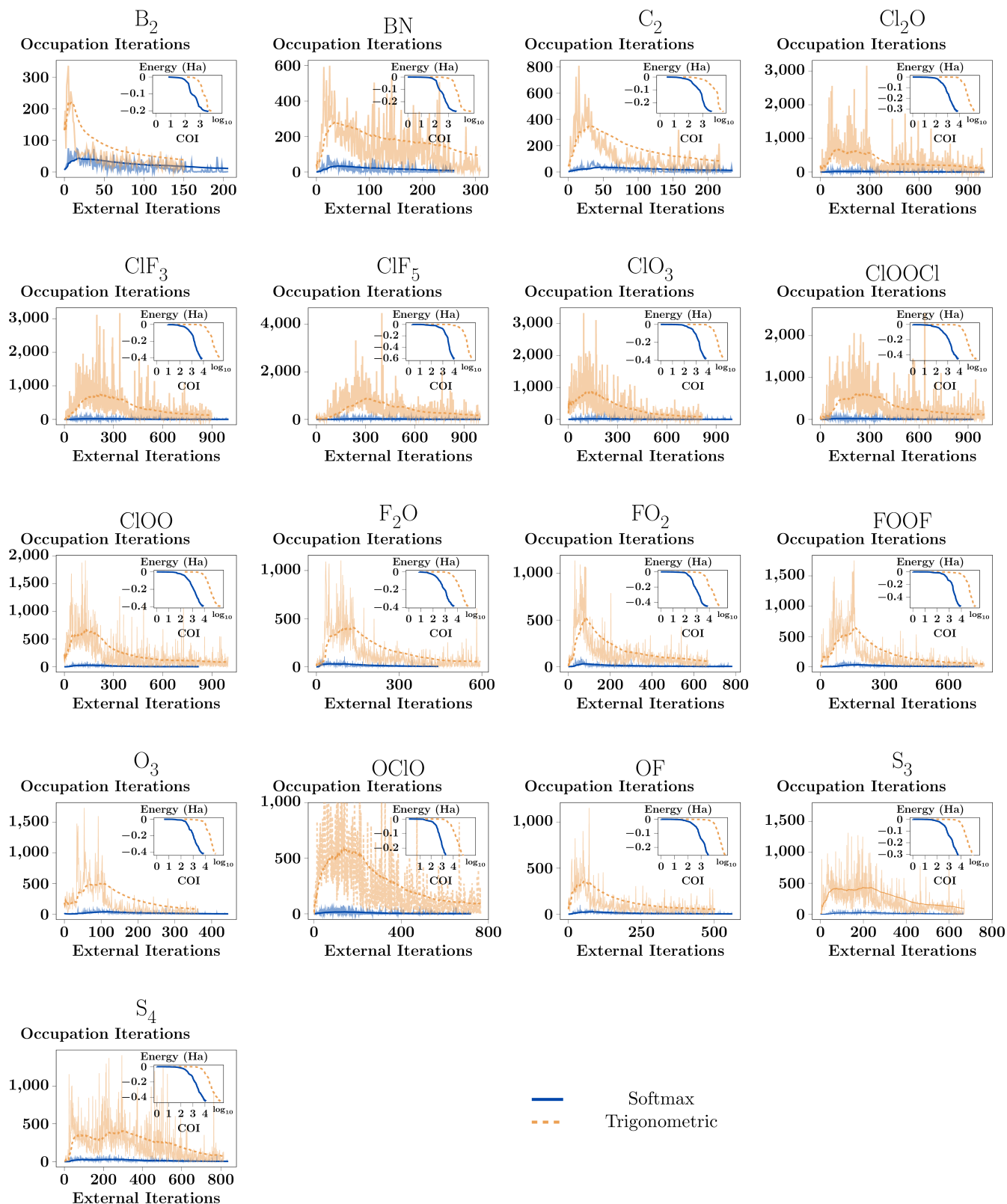


Figure 4: Representative calculation of the W4-17-MR set using the softmax (blue solid curves) and trigonometric (orange dashed curves) parameterization methods. The main panels illustrate the number of occupation iterations for each external iteration. The inset panels depict the energy relative to Hartree-Fock as a function of the cumulative occupation iterations (COI) on a logarithmic scale.

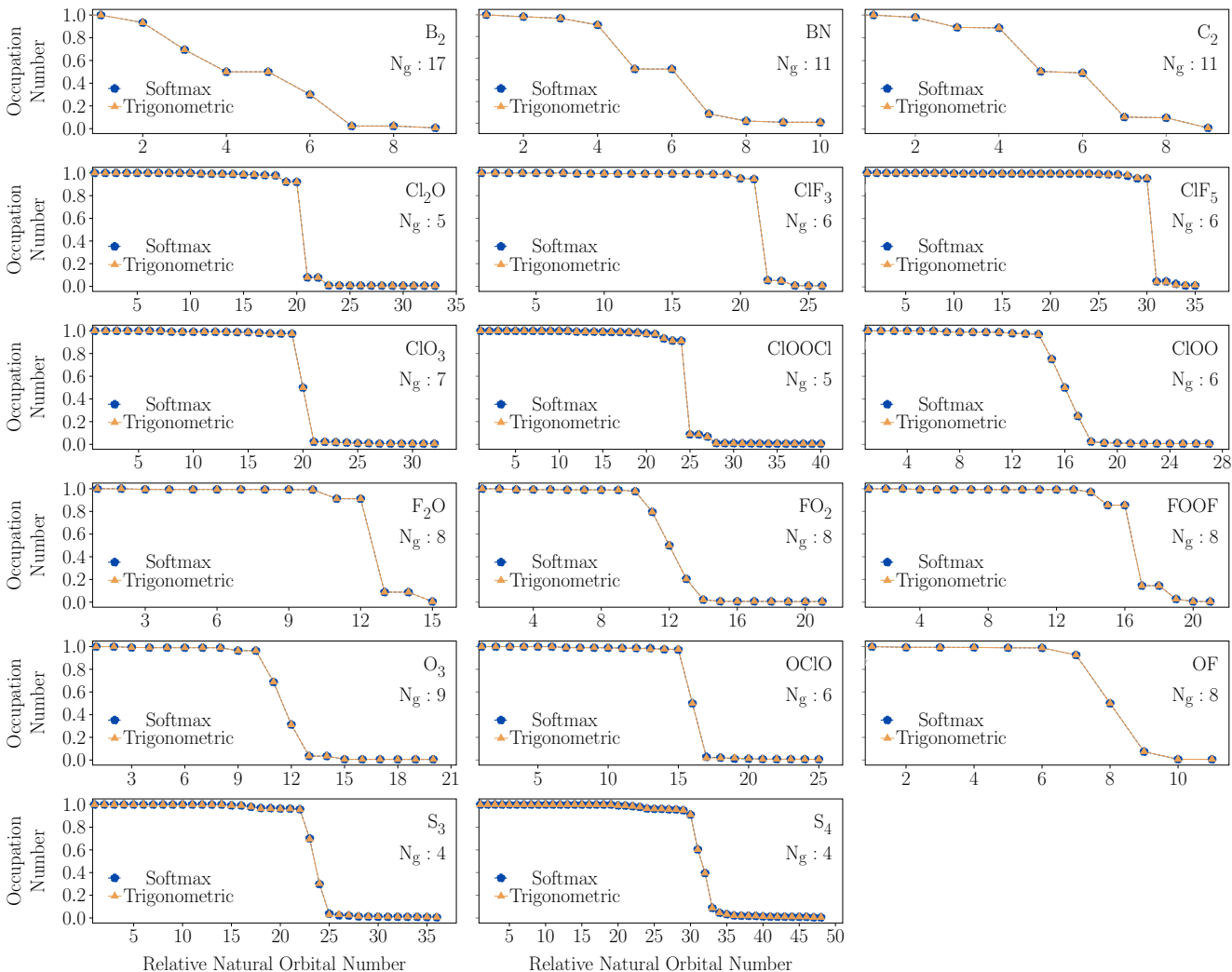


Figure 5: The ONs for each molecule in the W4-17-MR set were computed with both the frameworks - softmax (blue) and trigonometric (orange). These figures highlight the propensity of the ONs to cluster near one and zero.

counterpart. Compared to traditional parameterization methods, the COI panels also reveal that the softmax framework achieves energy convergence with fewer occupation iterations—ranging between one and two orders of magnitude less. Consequently, this indicates that softmax parameterization substantially enhances the overall optimization process.

The performance of the softmax parameterization can be explained by the ONs distribution, as presented in Figs. 3 and 5, where it can be seen that most ONs are close to one and zero, and only a few have values that are significantly fractional and close to $\frac{1}{2}$. This distribution is in good agreement with the concept of core and virtual orbitals, underscoring the existence of ONs firmly entrenched at the ex-

treme ends of the occupancy spectrum, even in a multireference set. In practice, only a few orbitals close to the highest occupied and the lowest unoccupied NO border exhibit deviations in their occupancy, with these fractional occupations becoming critical for strongly correlated systems. The observed distribution supports the adoption of sophisticated parameterization functions, such as the softmax function, from a data-driven perspective.

Finally, Fig. 6 displays the optimization results of ONs, starting from the already converged NOs, with the molecules indexed vertically. The markers' colors correspond to the M-diagnostic developed by Tishchenko *et al.*⁵⁷ and later adapted for the NOF framework.⁴⁰ This color coding illustrates the fractional occu-

pation levels in each system’s highest occupied natural orbital. Specifically, Fig. 6(a) compares the number of iterations required using the trigonometric and softmax parameterizations ($R_{T:S}$), demonstrating a reduction in iterations with the softmax approach across all molecules when the softmax parameterization is used. For this purpose, we define the $R_{T:S}$ ratio between the number of occupation iterations performed when using the trigonometric and softmax parameterization. Notably, the $R_{T:S}$ ratios are $\sim 2, 4,$ and 5 for $C_2, O_3,$ and $B_2,$ respectively, indicating enhanced convergence with the softmax parameterization, even in these smaller systems. Other molecules show greater acceleration, with the ratio of iterations ranging from 10 to 30, always in favor of the softmax parameterization. In addition, energy calculations using both frameworks reach comparable values. Fig. 6(b) plots the energy differences ($\Delta E = E_{\text{softmax}} - E_{\text{trigonometric}}$) along the horizontal axis, where a positive value indicates the trigonometric parameterization reached a lower energy value than the softmax parameterization. Although the softmax parameterization generally results in slightly higher energy values ($\Delta E > 0$), the maximum deviation is minimal, at only 0.0015 kcal/mol. Given the magnitude of these differences, we conclude that the softmax parameterization not only equates in energy to the trigonometric approach but also significantly reduces the number of iterations required, thus enhancing the stability of the optimization process for the ONs.

Conclusions

We have introduced an alternative methodology to parameterize the ONs of NOs, a critical component in 1RDMFT methodologies. Our approach leverages the softmax function, a key component in modern deep learning models, to ensure the N-representability constraint without the need for additional variables or complex constraint-optimization strategies. This new strategy significantly accelerates the convergence of PNOF calculations, achieving a 2 to 30-fold increase in speed compared to tradi-

tional parameterizations, such as trigonometric methods.

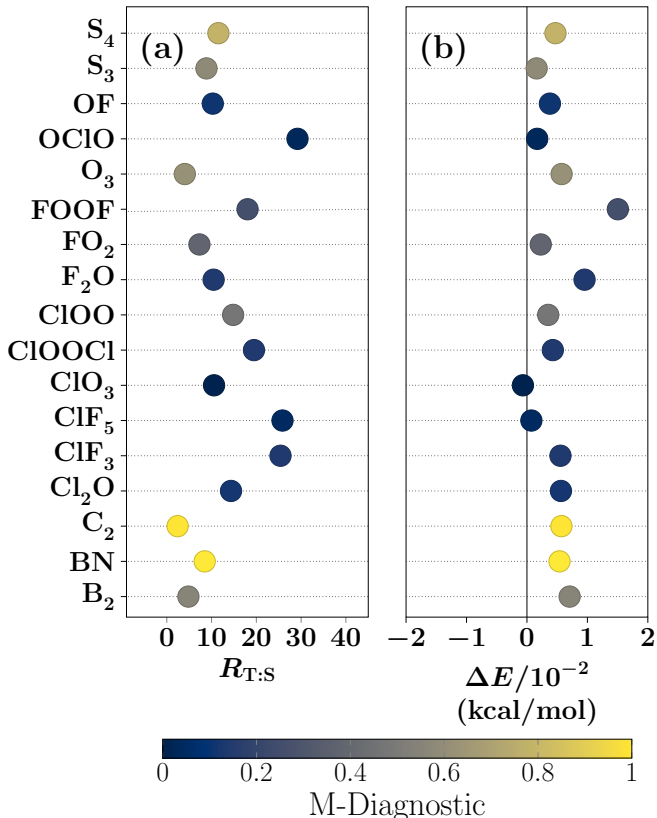


Figure 6: (a) The ratio between the trigonometric and softmax occupancy iterations, $R_{T:S}$. (b) The energy difference of occupancy optimization between both parameterizations, $\Delta E = E_{\text{softmax}} - E_{\text{trigonometric}}$, using the same converged set of orbitals for both parameterizations. Both panels are for each molecule of the W4-17-MR set with PNOF7. The color bar shows relative values of the M-diagnostic, which indicates the multireference nature of the systems.

This method has been validated on the W4-17-MR molecular dataset, known for its multireference character, demonstrating its effectiveness and efficiency. The success of this approach in handling the dataset’s complexities highlights its potential applicability across various 1RDMFT methodologies that require optimization of ONs. Moreover, the adoption of alternative parameterizations, such as softmax, could provide groundbreaking solutions to the intricate problems faced in quantum chemistry. This opens new avenues for enhancing com-

putational methodologies and tackling the demanding challenges within the RDMFT field.

Acknowledgement R. A. Vargas-Hernández acknowledges useful discussions with Chong Sun. M. Piris thanks the Eusko Jaurlaritza (Basque Government), Ref. No. : IT1584-22, for financial support, as well as Grant No. PID 2021-126714NB-I00, funded by Grant No. MCIN/AEI/10.13039/501100011033. J. F. H. Lew-Yee acknowledges the Donostia International Physics Center (DIPC) and the MCIN program “Severo Ochoa” under reference No. AEI/ CEX2018-000867-S for post-doctoral funding (Ref. No. : 2023/74). L. Franco with CVU Grant No. 1312732 acknowledges “Consejo Nacional de Humanidades, Ciencias y Tecnologías (CONAHCyT)” for a master scholarship. J. M. del Campo, L. Franco, and I. A. Bonfil-Rivera acknowledge funding with project Grant No. IN201822 from PAPIIT, and computing resources from “Laboratorio Nacional de Cómputo de Alto Desempeño (LANCAD)” with project Grant No. LANCAD-UNAMDGTIC-270.

References

- (1) Mazziotti, D. A. Quantum chemistry without wave functions: Two-electron reduced density matrices. *Acc. Chem. Res.* **2006**, *39*, 207–215.
- (2) Gilbert, T. L. Hohenberg-Kohn theorem for nonlocal external potentials. *Phys. Rev. B* **1975**, *12*, 2111–2120.
- (3) Hohenberg, P.; Kohn, W. Inhomogeneous electron gas. *Phys. Rev.* **1964**, *136*, B864–B871.
- (4) Levy, M. Universal variational functionals of electron densities, first-order density matrices, and natural spin-orbitals and solution of the v -representability problem. *Proc. Natl. Acad. Sci. U. S. A.* **1979**, *76*, 6062–6065.
- (5) Valone, S. M. Consequences of extending 1-matrix energy functionals from pure-state representable to all ensemble representable 1 matrices. *J. Chem. Phys.* **1980**, *73*, 1344–1349.
- (6) Coleman, A. J. Structure of fermion density matrices. *Rev. Mod. Phys.* **1963**, *35*, 668–686.
- (7) Löwdin, P.-O. Quantum theory of many-particle systems. I. Physical interpretations by means of density matrices, natural spin-orbitals, and convergence problems in the method of configurational interaction. *Phys. Rev.* **1955**, *97*, 1474–1489.
- (8) Müller, A. M. K. Explicit approximate relation between reduced two- and one-particle density matrices. *Phys. Lett. A* **1984**, *105*, 446–452.
- (9) Goedecker, S.; Umrigar, C. J. Natural orbital functional for the many-electron problem. *Phys. Rev. Lett.* **1998**, *81*, 866–869.
- (10) Gritsenko, O.; Pernal, K.; Baerends, E. J. An improved density matrix functional by physically motivated repulsive corrections. *J. Chem. Phys.* **2005**, *122*, 204102.
- (11) Piris, M. A new approach for the two-electron cumulant in natural orbital functional theory. *Int. J. Quantum Chem.* **2006**, *106*, 1093–1104.
- (12) Lathiotakis, N. N.; Marques, M. A. L. Benchmark calculations for reduced density-matrix functional theory. *J. Chem. Phys.* **2008**, *128*, 184103.
- (13) Schilling, C. Communication: Relating the pure and ensemble density matrix functional. *J. Chem. Phys.* **2018**, *149*, 231102.
- (14) Schilling, C.; Schilling, R. Diverging exchange force and form of the exact density matrix functional. *Phys. Rev. Lett.* **2019**, *122*, 013001.

- (15) Schilling, C.; Pittalis, S. Ensemble reduced density matrix functional theory for excited states and hierarchical generalization of Pauli’s exclusion principle. *Phys. Rev. Lett.* **2021**, *127*, 023001.
- (16) Liebert, J.; Castillo, F.; Labbé, J.-P.; Schilling, C. Foundation of one-particle reduced density matrix functional theory for excited states. *J. Chem. Theory Comput.* **2022**, *18*, 124–140.
- (17) Cioslowski, J.; Schilling, C.; Schilling, R. 1-matrix functional for long-range interaction energy of two hydrogen atoms. *J. Chem. Phys.* **2023**, *158*, 084106.
- (18) Castillo, F.; Labbé, J.-P.; Liebert, J.; Padrol, A.; Philippe, E.; Schilling, C. An effective solution to convex 1-body N-representability. *Ann. Henri Poincaré* **2023**, *24*, 2241–2321.
- (19) Liebert, J.; Chaou, A. Y.; Schilling, C. Refining and relating fundamentals of functional theory. *J. Chem. Phys.* **2023**, *158*, 214108.
- (20) Piris, M. Advances in approximate natural orbital functionals: From historical perspectives to contemporary developments. *Adv. Quantum Chem.* **2024**, *90*, 1–61.
- (21) Piris, M.; Ugalde, J. M. Iterative diagonalization for orbital optimization in natural orbital functional theory. *J. Comput. Chem.* **2009**, *30*, 2078–2086.
- (22) Herbert, J. M.; Harriman, J. E. N-representability and variational stability in natural orbital functional theory. *J. Chem. Phys.* **2003**, *118*, 10835–10846.
- (23) Elayan, I. A.; Gupta, R.; Hollett, J. W. Δ NO and the complexities of electron correlation in simple hydrogen clusters. *J. Chem. Phys.* **2022**, *156*, 094102.
- (24) Baldsiefen, T.; Gross, E. K. U. Minimization procedure in reduced density matrix functional theory by means of an effective noninteracting system. *Comput. Theor. Chem.* **2013**, *1003*, 114–122.
- (25) Piris, M. A generalized self-consistent-field procedure in the improved BCS theory. *J. Math. Chem.* **1999**, *25*, 47–54.
- (26) Piris, M.; Mitxelena, I. DoNOF: An open-source implementation of natural-orbital-functional-based methods for quantum chemistry. *Comput. Phys. Commun.* **2021**, *259*, 107651.
- (27) Yao, Y.-F.; Fang, W.-H.; Su, N. Q. Handling ensemble N-representability constraint in explicit-by-implicit manner. *J. Phys. Chem. Lett.* **2021**, *12*, 6788–6793.
- (28) Yao, Y.-F.; Zhang, Z.; Fang, W.-H.; Su, N. Q. Explicit-by-implicit treatment of natural orbital occupations using first- and second-order optimization algorithms: A comparative study. *J. Phys. Chem. A* **2022**, *126*, 5654–5662.
- (29) Cartier, N. G.; Giesbertz, K. J. H. Exploiting the Hessian for a better convergence of the SCF-RDMFT procedure. *J. Chem. Theory Comput.* **2024**, *20*, 3669.
- (30) Yao, Y.-F.; Su, N. Q. Enhancing reduced density matrix functional theory calculations by coupling orbital and occupation optimizations. 2024.
- (31) Shao, X.; Paetow, L.; Tuckerman, M. E.; Pavanello, M. Machine learning electronic structure methods based on the one-electron reduced density matrix. *Nat. Commun* **2023**, *14*, 6281.
- (32) Sager-Smith, L. M.; Mazziotti, D. A. Reducing the quantum many-electron problem to two electrons with machine learning. *J. Am. Chem. Soc.* **2022**, *144*, 18959–18966.
- (33) Jones, G. M.; Li, R. R.; DePrince, A. E. I.; Vogiatzis, K. D. Data-driven refinement of electronic energies from two-electron reduced-density-matrix theory. *J. Phys. Chem. Lett.* **2023**, *14*, 6377–6385.
- (34) Dawid, A.; Arnold, J.; Requena, B.; Gresch, A.; Płodzień, M.; Donatella, K.;

- Nicoli, K. A.; Stornati, P.; Koch, R.; Büttner, M. et al. Modern applications of machine learning in quantum sciences. 2023.
- (35) Kunc, V.; Kléma, J. Three decades of activations: A Comprehensive Survey of 400 activation functions for neural networks. 2024.
- (36) Piris, M.; Lopez, X.; Ruipérez, F.; Matxain, J. M.; Ugalde, J. M. A natural orbital functional for multiconfigurational states. *J. Chem. Phys.* **2011**, *134*, 164102.
- (37) Piris, M.; Matxain, J. M.; Lopez, X. The intrapair electron correlation in natural orbital functional theory. *J. Chem. Phys.* **2013**, *139*, 234109.
- (38) Piris, M. Interacting pairs in natural orbital functional theory. *J. Chem. Phys.* **2014**, *141*, 044107.
- (39) Piris, M. Global method for electron correlation. *Phys. Rev. Lett.* **2017**, *119*, 063002.
- (40) Lew-Yee, J. F. H.; M Del Campo, J. Charge delocalization error in Piris natural orbital functionals. *J. Chem. Phys.* **2022**, *157*, 104113.
- (41) Huan Lew-Yee, J. F.; Piris, M.; Del Campo, J. M. Outstanding improvement in removing the delocalization error by global natural orbital functional. *J. Chem. Phys.* **2023**, *158*, 084110.
- (42) Mitxelena, I.; Piris, M. Benchmarking GNOF against FCI in challenging systems in one, two, and three dimensions. *J. Chem. Phys.* **2022**, *156*, 214102.
- (43) Mercero, J. M.; Grande-Aztatzi, R.; Ugalde, J. M.; Piris, M. In *Chapter Thirteen - Natural orbital functional theory studies of all-metal aromaticity: The Al₃⁻ anion*; Hoggan, P. E., Ed.; Advances in Quantum Chemistry; Academic Press, 2023; Vol. 88; pp 229–248.
- (44) Lew-Yee, J. F. H.; del Campo, J. M.; Piris, M. Electron correlation in the iron(II) porphyrin by natural orbital functional approximations. *J. Chem. Theory Comput.* **2023**, *19*, 211–220.
- (45) Franco, L.; Lew-Yee, J. F. H.; M. del Campo, J. Correlation balance for describing carbenes: An NOF study. *AIP Adv* **2023**, *13*, 065213.
- (46) Piris, M. Global natural orbital functional: Towards the complete description of the electron correlation. *Phys. Rev. Lett.* **2021**, *127*, 233001.
- (47) Lew-Yee, J. F. H.; Piris, M.; M. del Campo, J. Resolution of the identity approximation applied to PNOF correlation calculations. *J. Chem. Phys.* **2021**, *154*, 064102.
- (48) Piris, M. Natural orbital functional for multiplets. *Phys. Rev. A* **2019**, *100*, 032508.
- (49) Piris, M. In *Theoretical and Quantum Chemistry at the Dawn. 21st Century*; Chakraborty, T., Carbó-Dorca, R., Eds.; Apple Academic Press, 2018; Chapter 22, pp 593–620.
- (50) Bridle, J. S. Training stochastic model recognition algorithms as networks can lead to maximum mutual information estimation of parameters. Proceedings of the 2nd International Conference on Neural Information Processing Systems. Cambridge, MA, USA, 1989; p 211–217.
- (51) Vargas-Hernández, R. A.; Jorner, K.; Pollice, R.; Aspuru-Guzik, A. Inverse molecular design and parameter optimization with Hückel theory using automatic differentiation. *J. Chem. Phys.* **2023**, *158*, 104801.
- (52) Lemke, Y.; Kussmann, J.; Ochsenfeld, C. Efficient integral-direct methods for self-consistent reduced density matrix functional theory calculations on central and

- graphics processing units. *J. Chem. Theory Comput.* **2022**, *18*, 4229–4244.
- (53) Lew-Yee, J. F. H.; Piris, M.; M. del Campo, J. PyNOF. <https://github.com/felipelewyee/PyNOF>, 2024.
- (54) Weigend, F.; Ahlrichs, R. Balanced basis sets of split valence, triple zeta valence and quadruple zeta valence quality for H to Rn: Design and assessment of accuracy. *Phys. Chem. Chem. Phys.* **2005**, *7*, 3297–3305.
- (55) Rappoport, D.; Furche, F. Property-optimized Gaussian basis sets for molecular response calculations. *J. Chem. Phys.* **2010**, *133*, 134105.
- (56) Karton, A.; Sylvetsky, N.; Martin, J. M. L. W4-17: A diverse and high-confidence dataset of atomization energies for benchmarking high-level electronic structure methods. *J. Comput. Chem.* **2017**, *38*, 2063–2075.
- (57) Tishchenko, O.; Zheng, J.; Truhlar, D. G. Multireference model chemistries for thermochemical kinetics. *J. Chem. Theory Comput.* **2008**, *4*, 1208–1219.